Title: Improvement of human donor retinal ganglion cell survival through modulation of microglia

Volha V. Malechka[1], Monichan Hayes Phay[1*], Josy Augustine[1,2], Emil Kriukov[1], John Dayron Rivera[1], Clemens Alt[3], Meredith Gregory-Ksander[1], Petr Baranov[1]*

[1]Department of Ophthalmology, Schepens Eye Research Institute of Massachusetts Eye and Ear, Harvard Medical School, Boston, Massachusetts, USA 02114

[2]Wellcome-Wolfson Institute for Experimental Medicine, School of Medicine, Dentistry and Biomedical Sciences, Queen's University Belfast, Belfast, United Kingdom

[3]Center for Systems Biology and Wellman Center for Photomedicine, Massachusetts General Hospital and Harvard Medical School, Boston, Massachusetts, USA

*Contributed equally

Running Head: Improvement of donor hRGCs survival through microglia modulation

Correspondence: Petr_Baranov@meei.harvard.edu

Conflict of Interests: No conflicting relationship exists for any author

Financial Support: NEI/NIH U24 (PB), GFF (PB), DoD FTTSA VRP (PB), Gilbert Family Foundation (PB)

Keywords: transplantation, microglia, retinal ganglion cells, stem cell therapy, soluble Fas ligand, annexin V

Abstract

Stem cell-derived retinal ganglion cell transplantation therapy offers a promising avenue for restoring vision in patients with significant retinal ganglion cell loss. The major challenge in this therapeutic approach is ensuring the survival of transplanted human donor retinal ganglion cells within the host retina. Here, we demonstrated the pivotal role of host retinal microglia and macrophages in the rejection, acceptance and survival of human donor cells. To identify the potential targets for treatment in microglia-retinal ganglion cell interaction, we assembled a single-cell atlas for mouse retina during development, aging, maturation and across neurodegenerative conditions. To our knowledge, this is the largest integrated atlas containing 1,053,629 cells including 36,080 myeloid cells. The downstream analysis highlighted phagocytosis among other known pathways involved in microglia activation, neuroinflammation and host retinal ganglion cell damage. We hypothesized that the same mechanisms are responsible for donor retinal ganglion cell removal. We showed that it is possible to improve the survival of human donor stem cell-derived retinal ganglion cells through modulation of the host retinal microglia. Pretreatment of human donor retinal ganglion cells with annexin V and/or soluble Fas ligand before transplantation led to a 2.5-fold increase in donor cell survival, including the outgrowth of axons targeting optic nerve head. Detailed analyses of the host mouse retina post-transplantation revealed morphological changes microglia and macrophages typical for activation in neuroinflammation. These findings indicate that soluble Fas ligand and annexin V treatment can be used to improve the success rate of transplantation of neurons within the retina and central nervous system.

Introduction

The degeneration of retinal ganglion cells (RGCs) is a key factor in various eye disorders, including different forms of glaucoma, hereditary optic neuropathies, ischemic optic neuropathies, and demyelinating diseases, all of which result in progressive axonal degeneration and death of RGCs, ultimately leading to irreversible blindness. [1–5] Despite significant advances, the clinical needs for these retinal neurodegenerative conditions remain largely unmet. Consequently, a variety of therapeutic strategies are being actively explored, including cell replacement therapy, pharmacologic neuroprotection, and gene therapy. [6–9] Among these, stem cell-derived RGC transplantation therapy holds considerable promise for restoring vision in patients with RGC loss and axonal degeneration. [10,11] One of the primary challenges with this therapeutic approach is ensuring the survival of the transplanted human RGCs within the host retina. In the majority of neuron transplantation studies, the survival rate remains below 10% and is generally attributed to donor cell death due to shear stress and mechanical damage, lack of trophic factors, hypoxia, several cell death mechanisms and activation of innate and adaptive immune responses. [12–14] In this study, we explored the contribution of microglia, the major effector cell of the innate retinal immune system, to the survival rate of donor human retinal ganglion cells (hRGCs) following transplantation. [15]

In the healthy and normally developed retina, microglia reside in the outer plexiform layer (OPL) and inner plexiform layer (IPL), where they perform essential functions in immune defense, homeostasis, and development. [16] When exposed to damaging stimuli, microglia become activated and migrate to the sites of retinal injury, where they can become neurotoxic and eliminate damaged and stressed RGCs. [17,18] We hypothesize that the

70 similar process happens in host retina microglia and macrophages after transplantation
71 of donor RGCs. To identify the potential targets for treatment in microglia-RGC
72 interaction, we assembled a single-cell atlas for mouse retina during development, aging,
73 maturation and across neurodegenerative conditions. To our knowledge this is the largest
74 integrated atlas containing 1,053,629 cells including 36,080 myeloid cells. The
75 downstream analysis confirmed previous observations of similar pathways in microglia
76 activation and highlighted the role of phagocytosis as a universal response to damage.
77 We hypothesize that during cell isolation and transplantation, donor hRGCs undergo
78 significant stress, which leads to the externalization of pro-apoptotic signals on their cell
79 surface. [19] These signals attract tissue microglia and macrophages to the site of injury
80 and initiate phagocytosis of the transplanted cells. By blocking these signals and
81 modulating the host retinal microenvironment, we aim to prevent microglia and
82 macrophages from recognizing and eliminating the transplanted cells, thereby enhancing
83 the survival of donor hRGCs post-transplantation.
84 Annexin V emerges as a potential candidate for modulating the retinal microenvironment
85 and preventing microglia and macrophages from recognizing and removing donor hRGCs
86 after transplantation. Annexin V is a calcium-dependent, membrane-bound protein with
87 high affinity for phosphatidylserine (PS), an endogenous phospholipid and a component
88 of the plasma membrane that becomes exposed on the cell surface during cellular stress
89 and early apoptosis. Given the distressing nature of isolation and transplantation, donor
90 hRGCs likely externalize PS under stress. Therefore, we hypothesized that pretreating
91 donor hRGCs with annexin V to mask PS would prevent recognition and clearance by
92 microglia and macrophages following transplantation.

93 Fas ligand (FasL), or CD95 ligand, is another possible candidate for modulating the retinal
94 microenvironment and improving survival of transplanted donor hRGCs. FasL is a 40kDa
95 type II transmembrane protein of the tumor necrosis factor (TNF) family that is capable of
96 inducing apoptosis upon binding to the Fas receptor. [20] Within the eye, FasL can be
97 expressed as a membrane-bound protein (mFasL), which is pro-inflammatory and pro-
98 apoptotic molecule, or cleaved and released as a soluble protein (sFasL), which is non-
99 inflammatory and non-apoptotic. [21,22] Previous studies demonstrated that FasL deficiency
100 or intravitreal administration of sFasL protects RGCs from cell death in a mouse model of
101 glaucoma. [23] Furthermore, sFasL has demonstrated therapeutic benefits in reducing
102 inflammation in experimental models of keratitis[24] and autoimmune disease. [25] Thus, we
103 hypothesize that Fas-FasL interaction may protect donor hRGCs from immune attack by
104 host microglia and macrophages, thereby improving graft survival in the host retina.
105 Taken together, this study demonstrates that pretreating donor hRGCs with annexin V
106 and sFasL before transplantation modulates the host microenvironment and improves
107 graft survival in the host mouse retina. Additionally, our results provide the first
108 quantitative analysis of microglia and macrophages morphology in the mouse retina
109 following donor hRGC transplantation.
110

111 **Materials and methods**

112 **Animals**

113 All procedures conformed to the National Research Council's Guide for the Care and Use
114 of Laboratory Animals, the Association for Research in Vision and Ophthalmology
115 (ARVO) guidelines and were approved by the Institutional Animal Care and Use

116 Committee (IACUC) of the Schepens Eye Research Institute (SERI). All animals were
117 purchased from Jackson Laboratory (Bar Harbor, ME). The breeding of animals was
118 established in the Rodent Barrier Facility at the SERI. At the beginning of the experiment
119 equal numbers of male and female *Brn3b*$^{-/-}$ and *Cx3cr1*$^{GFP/+}$ on a C57BL/6J background
120 mice were group-housed in a temperature-controlled environment with 12-hour light/dark
121 cycle and received a standard diet and water ad libitum.
122

123 **Organoid dissociation and isolation of donor hRGCs**

124 Retinal ganglion cells (RGCs) were differentiated from H9:BRN3B:tdTomatoThy1.2-
125 hESCs in 3D retinal organoid culture, as was previously described.[26–28] Mature human
126 retinal organoids were dissociated, and RGCs were isolated using magnetic microbead
127 sorting for Thy1.2+ cells. Following cell isolation, RGCs were formulated in RGC media
128 at 1 – 5 x 10^5 cells/mL. Then, donor hRGCs were pretreated with 5 mg/mL annexin V
129 (BioLegend, San Diego, CA), a calcium-dependent membrane-bound protein with high
130 affinity to PS, and 0.2 mg/mL sFasL (R&D Systems, Minneapolis, MN), a non-apoptotic,
131 non-inflammatory protein, for at least 20 minutes on ice. Following donor hRGC
132 pretreatment, the cells were formulated for transplantation at 2 x 10^4 cell/μL in RGC
133 media.
134

135 ***In vivo* transplantation of donor hRGCs**

136 The *Brn3b*$^{-/-}$ mice were anesthetized intraperitoneally with 100 mg/kg ketamine
137 hydrochloride and 20 mg/kg xylazine hydrochloride solution diluted with saline. Pupils
138 were dilated with 1% tropicamide ophthalmic solution (Bausch + Lomb, Bridgewater, NJ).

139 Following tropicamide application, one drop of 0.5% proparacaine hydrochloride
140 ophthalmic solution (Bausch + Lomb, Bridgewater, NJ) was applied onto the cornea for 5
141 minutes before transplantation. Up to 2 x 10^4 donor cells per 1 μL were injected into one
142 eye of *Brn3b*$^{-/-}$ mice using a beveled glass microneedle with 100 μm inner diameter at a
143 1 μL/min flow rate. Each mouse received a single subretinal injection of 1.0 μL of donor
144 hRGCs pretreated with annexin V and sFasL during transplantation. Control group
145 received a single subretinal injection of 1.0 μL of donor hRGCs with no annexin V or
146 sFasL pretreatment. Following donor hRGC transplantation, one drop of GenTeal® Tears
147 Lubricant eye gel (Alcon Laboratories, Fort Worth, TX) was applied onto the cornea to
148 protect the eye from dryness. Mice were returned to the housing room and maintained on
149 a standard 12-hour light/dark cycle for 3 days. On day 3 mice were euthanized, and eyes
150 were immediately collected and fixed in 4 % paraformaldehyde (PFA) for 12 hours before
151 immunohistochemistry analysis.
152
153 **Immunostaining of whole mount retinas**
154 After fixation with 4% PFA was complete, retina samples were incubated in blocking
155 buffer [10 % goat serum, 1 % bovine serum albumin (BSA), 0.1 % sodium citrate, 0.1 %
156 Tween 20, and 0.1 % Triton-X in 1X phosphate-buffered saline (PBS)] containing goat
157 anti-mouse antibodies in dilution 1:400 at 4°C for at least 12 hours overnight to limit
158 nonspecific staining. Following blocking, retina flat mounts were incubated with Iba-1
159 primary antibodies (ab178846, Abcam, Boston, MA) in staining buffer (1 % BSA, 0.25 %
160 Tween 20 and 0.25 % Triton-X in 1X PBS) for 72 hours at 4°C. Then, each retina sample
161 was washed thrice for 15 minutes with washing buffer (0.1 % Tween-20, 0.1 % Triton-X

162 in 1X PBS) at room temperature to remove any unbound primary antibodies before adding
163 secondary antibodies. Secondary antibodies were prepared in dilution 1:500 in staining
164 buffer, and the retina samples were incubated with secondary antibodies for 24 hours at
165 4°C. Then, each sample was washed with washing buffer thrice for 15 minutes at room
166 temperature and then incubated with 1 μg/mL DAPI (4',6-diamidino-2-phenylindole) in 1X
167 PBS for 20 minutes at room temperature to stain the cell nuclei. Following final rinse with
168 1X PBS, retina samples were mounted and stored in the dark at room temperature before
169 imaging. Images of retina mounts were acquired using confocal microscope (Olympus,
170 Tokyo, Japan), and the Iba1$^+$ microglia and macrophages were imaged within the OPL
171 and IPL.
172

173 **Morphometric analysis of Iba1$^+$ microglia and macrophages**

174 The image of each retina flat mount was divided into four quadrants with one mid-
175 peripheral region being a representative image of each quadrant; therefore, a total of four
176 images per retina was used for quantitative analysis of retinal microglia and
177 macrophages. The analysis was applied to quantify retinal microglia and macrophages
178 and assess morphology of retinal microglia and macrophages according to metrics such
179 as cell shape, ramification, and complexity. Morphology analysis of total number of Iba1$^+$
180 retinal microglia and macrophages within the OPL and IPL was performed on
181 skeletonized images of Iba1$^+$ cells from the retinal flat mounts using previously published
182 protocols. [29] Briefly, eight Z-stack images (two images per retinal quadrant) were captured
183 at 20X magnification from one retina per animal and processed using ImageJ software
184 (provided in the public domain). The images were binarized using the "adjust threshold"

185 function and skeletonized using the “skeletonize” function. The plugin “Analyze Skeleton”
186 was then employed to generate the number of branches, number of junctions, and
187 average branch length of the microglia and macrophages in the retina flat mounts. All
188 morphometric parameter values were divided by the total number of cells per unit area of
189 retinal tissue in mm^2.
190

191 **Single-cell RNA-sequencing data analysis**

192 Data analysis was performed using R v.4.3.1 in RStudio 2023.06.1 Build 524. To perform
193 reference mapping and multi conditional RGC/myeloid studies, we compiled multiple
194 publicly available datasets for the conditions such as mouse healthy developing retina,
195 mouse healthy adult retina, mouse optic nerve crush model, and mouse glaucoma model
196 retina. The complete list of publicly available datasets used in this study is available in
197 **Supplementary Table 1**. Cell ranger outputs that include matrix, features, and barcodes
198 were obtained from public GEO repositories, and further processed using Seurat v.
199 4.3.0.1. (Hao Y et al. Nat Biotechnol, 2023; Hao Y et al. Cell, 2021) Quality control metrics
200 included filtering by nCount_RNA, nFeature_RNA, percent.mt, percent.rb. Doublets were
201 removed using the DoubletFinder algorithm. (McGinnis CS et al, Cell Syst, 2019) Each
202 dataset was processed independently for the quality control and data processing,
203 followed by conditional integration that was performed using multiple approaches: 1)
204 default Seurat integration, 2) Seurat RPCA-based integrated, 3) Harmony, (Korsunsky I
205 et al. Nat Methods, 2019) 4) scVI. (Lopez R et al. Nat Methods, 2018) The selection of
206 method was based on the number of batches, batches variation, and the number of cells.
207 Upon the integration, we subset RGC/myeloid from each condition and reintegrate the

208 resulting subsets into multi conditional RGC and myeloid atlases. Further downstream
209 analysis was performed using Seurat and escape v.1.10.0 packages. Pathways for GSEA
210 pathway analysis were obtained from Molecular Signatures Database.
211
212 **Results**
213 **RGC survival is improved following blocking phosphatidylserine residues with**
214 **annexin V on donor hRGCs**
215 Annexin V pretreatment led to the increase in transplant success: 92% (11 out of 12
216 recipients) had >1% (200) donor cells at day 4, compared to only 55% (6 out of 11) in the
217 control group. We also observed 2.5-fold change in number of donor RGCs per eye: with
218 mean numbers at 1,280 cells in pretreated vs. 520 cells in control. In both groups grafted
219 donor RGCs displayed extensive neurite outgrowth (>150 mm) and axon projections
220 (>1,000 mm) (**Figure 1A, B**). Furthermore, in the annexin V pretreated group, four out of
221 twelve transplants exhibited neurite outgrowth into the optic nerve head, compared to
222 only one out of eleven transplants in the control group (**Figure 1C**).
223
224 **Host microglia and macrophages are activated after donor hRGC transplantation**
225 **in *Cx3cr1-GFP* mice**
226 To study microglia activation *in vivo*, we imaged the retina repeatedly in *Cx3cr*$^{GFP/+}$ mice
227 by scanning laser ophthalmoscopy (SLO) [30] (**Figure 2**). On day 1 post-transplantation,
228 host retinal microglia and macrophages become activated and initiate displacement
229 toward injection site to remove the transplanted donor hRGCs (**Figure 2A, 2B**). By days
230 2 and 3, microglia and macrophages begin eliminating donor hRGCs, occupying the area

231 of damage, and by day 7 all donor hRGCs are removed and processed by microglia and
232 macrophages (**Figure 2A, 2B**).
233 Retinal microglia and macrophages rapidly respond to physiological changes and
234 demonstrate distinct morphology based on their state of reactivity. As shown in **Figure**
235 **2C,** activated microglia and macrophages retract their processes and round their cell
236 bodies, whereas in their homeostatic state they exhibit small cell bodies with ramified
237 processes.
238
239 **Donor hRGCs are eliminated by primary microglia *in vitro***
240 To determine if donor hRGCs are eliminated by microglia *in vitro*, we co-cultured primary
241 microglia with human donor RGCs (**Supplementary Figure 1A**). We have observed that
242 primary microglia become activated on day 1, move towards donor hRGCs, and begin
243 eliminating them by day 1 (**Supplementary Figure 1B**). This finding is consistent with
244 our observation *in vivo*, demonstrating that donor hRGCs are recognized and eliminated
245 by microglia in the host microenvironment. Therefore, modulating this microenvironment
246 might help suppress microglia activity and improve the survival of donor hRGCs.
247
248 **Activation of host microglia and macrophages is modified following exogenous**
249 **pretreatment of donor hRGCs with annexin V and sFasL**
250 To investigate whether the host retinal microenvironment, where microglia and
251 macrophages play an essential role in active surveillance can be modulated, we
252 pretreated donor hRGCs before transplantation. Following dissociation and isolation of
253 donor hRGCs, we pretreated the cells with 5 mg/mL annexin V and 0.2 mg/mL sFasL for

254 at least 20 minutes on ice. Following transplantation, our results indicate improved
255 survival and axonal elongation in donor hRGCs pretreated with annexin V and sFasL as
256 compared to non-pretreated cells (**Figure 3A, 3B**).
257 Microglia are resident cells in the retina localized in two distinct layers within OPL and IPL
258 in the intact retina. [31] To explore the effect of pretreating donor hRGCs with annexin V
259 and sFasL on microglia and macrophages, we analyzed Iba1^{+} cells within OPL and IPL
260 after donor hRGC transplantation. At 3 days post transplantation of donor hRGCs
261 pretreated with Annexin V and sFasL, microglia and macrophages displayed homeostatic
262 morphology with prominent and longer processes as compared to the control group with
263 no pretreatment, where microglia and macrophages displayed a more reactive phenotype
264 with rounded cell bodies and retracted processes (**Figures 3C-F**). Interestingly, we also
265 found that microglia and macrophages become more activated in the OPL as compared
266 to the IPL after subretinal delivery of donor hRGCs (**Figures 3C-F**). Moreover, the total
267 number of microglia and macrophages was reduced in the pretreatment group as
268 compared to the control group with no pretreatment (**Figures 3G, 3J**), again with more
269 significant changes observed in IPL. Additionally, the number of branches per microglia
270 and macrophage was significantly (p<0.01) increased in the pretreatment group,
271 indicating less activation when compared to the control group (no pre-treatment) (**Figures**
272 **3H, 3K**).
273 Moreover, microglia and macrophages in the OPL exhibit a significant difference in
274 branch number per cell between pretreated and control groups (**Figure 3H**), while those
275 in the IPL showed lower branch numbers per cell (**Figure 3K**). Similar trend is observed
276 in the branch length per microglia and macrophage cell with longer and more ramified

277 branches in OPL that in IPL, suggesting that microglia and macrophages are less
278 activated in the OPL than IPL after donor hRGC transplantation (**Figures 3I, 3L**).
279 In summary, pretreating donor hRGCs with annexin V and sFasL leads to morphologic
280 changes in microglia and macrophages within the OPL and IPL of the mouse retina.
281

282 **Characteristics of RGCs and microglia vary in the conditions of healthy developing,**
283 **adult, acute and chronic post-injury retina**

284 We built an atlas of microglia and macrophages from healthy developing retina, adult
285 retina, optic nerve crush (ONC) retina, and microbeads-induced glaucoma model retina
286 (**Figure 4A**) to better understand the process of neuroinflammation and the interaction of
287 activated microglia with the retinal neurons. While some condition-specific states are
288 present for developing microglia/macrophage, most clusters overlap between the
289 conditions. However, the differences are observed when assessing the classical
290 microglia-related genes expression (**Figure 4B**), where microglia and macrophages in
291 the developing retina are mostly characterized by strong proliferation, expression of
292 *Igfbpl1*, (Pan L et al. Cell Reports, 2023) *Ager*, and *Igf1*, and healthy adult retina state is
293 profiled by *Stab2* and *P2ry12*. In ONC retina, we first observe low expression of *P2ry12*,
294 a classic homeostatic microglia marker, that tends to increase over time. In addition, early
295 timepoints in ONC retina are characterized by *Stab1* and *Ccl4* with higher expression of
296 *Ccl5* week 2 post-ONC. Interestingly, we observe *Cdc20* and *Mki67* expression on days
297 2 and 4 post-ONC and an increase in *Apoe* expression on day 4 post-ONC. Retina in
298 microbeads-induced glaucoma model is characterized by *Timd4* and *Olr1* expression
299 demonstrating the pattern of increased *Cd74* expression compared to developing and

300 healthy adult retinas. FasL expression is the lowest in developing retina, whereas the
301 highest expression of FasL is observed in healthy adult and 2 weeks post-ONC retinas.
302 These patterns demonstrate a complicated scheme of microglia activation between
303 different conditions. To further inspect the conditional changes, we performed pathway
304 analysis using the pathways related to microglia activation (**Figure 4C**). As expected, we
305 observe myeloid progenitor cell differentiation to be the highest in developing retina.
306 Within all pathways related to microglia activation, we see healthy adult condition to have
307 the lowest enrichment score when compared to ONC and microbeads-induced glaucoma
308 model conditions. The number of differences exists between microglia activation in ONC
309 and microbeads-induced glaucoma model. ONC retina is characterized by higher
310 microglia proliferation, migration, and differentiation, whereas microbeads-induced
311 glaucoma model condition demonstrates a higher enrichment score in acute inflammatory
312 response and innate immune response activation.
313 As we observe such drastic differences in microglia activation between the conditions, we
314 explored the role of *Apoe,* one of the most variable markers in the conditions studied, in
315 microglia activation. Overall, we observed three peaks in *Apoe* expression in the
316 integrated dataset. The first peak shows *Apoe* cells, while the other two highlight *Apoe*$^{+}$
317 cells that for simplicity we call *Apoe*^{dim} and *Apoe*^{bright} (**Figure 4D**). Interestingly, the
318 distribution of *Apoe* expression is different between the conditions. Microglia in
319 developing retina demonstrates almost complete absence of the first peak of *Apoe*$^{-}$ cells,
320 and microglia in ONC retina >4 days has the distribution shifted towards higher
321 expression compared to ONC <=4 days condition (**Figure 4E**).

322 We further subset the *Apoe*^{bright} population with the threshold of expression set to ≥ 4. We
323 observe multiple trends in change of *Apoe*^{bright} population: 1) the population is growing
324 from healthy developing to healthy adult condition; 2) in the ONC timeline, the population
325 is growing up to week 1 post-ONC, then decreasing; 3) glaucoma model condition
326 population is similar to healthy adult retina (**Figure 4F**).
327 To understand the role of *Apoe* in microglia activation and to establish, whether it is a
328 marker of increased microglia activation or a marker of cells undergoing transition from
329 homeostatic to activated state, we compared datasets of average *Apoe* expression within
330 two populations - total integrated microglia/macrophage population and *Apoe*^{bright}
331 population (**Figure 4G**). Noticeably, *Apoe* expression does not change in *Apoe*^{bright}
332 population. For the total integrated microglia/macrophage population, average *Apoe*
333 expression decreases from developing to adult condition and is similar between the adult
334 and glaucoma model conditions. In the ONC condition, it increases up to week 1 post-
335 ONC.
336 In the same manner we integrated the multi conditional (developing, adult, and ONC) data
337 for RGCs (**Figure 5A**). We analyzed canonical “eat-me”, “do-not-eat-me”, and “find-me”
338 signaling markers between the conditions (**Figure 5B**). Healthy developing RGCs can be
339 profiled by *Lrp8* and *Rab5a* expression. Healthy adult RGCs express *Rab5a*, however,
340 they lose *Lrp8* expression. They are also characterized by *Cd93*, *Timd4*, *Stab2*, and *Tulp1*
341 expression, demonstrating a similar pattern to 2 weeks post-ONC condition. The timeline
342 of post-ONC condition can be separated into two functional timepoints, such as <=4 days
343 and >4 days, where <=4 days RGCs are positive for *Rab7*, *Cd47*, *Adgrb1*, and *Cx3cl1*,

344 while >4 days are positive for *Rab35*, *Gas6*, *Plscr3*, and *Spp1*. Noticeably, RGCs stand
345 separately and are positive for the majority of “eat-me” markers week 2 post-ONC.
346

347 **Discussion**

348 Optic neuropathies and retinal neurodegenerative diseases, such as glaucoma, diabetic
349 retinopathy, and age-related macular degeneration, result in progressive damage of
350 retinal ganglion cells (RGCs). [32] If left untreated, these diseases lead to irreversible
351 blindness. For the patients with optic neuropathies and neurodegenerative diseases of
352 the retina, cell replacement therapy [33–35] and treatment with neuroprotective agents are
353 promising strategies to halt disease progression and preserve vision.[36,37] One of the key
354 steps for improving cell transplantation success in the retina is to define the factors that
355 positively affect survival of donor RGCs and to modulate the host microenvironment [38] by
356 enhancing the beneficial effect of these factors on donor cells.
357 The retina is populated by specialized immune resident macrophages called microglia.
358 Normally, retinal microglia reside within the outer plexiform layer (OPL), the inner
359 plexiform layer (IPL), and the retinal ganglion cell (RGC) layer. Microglia represent one
360 of the main barriers the donor cells need to overcome for successful survival and
361 integration within the host microenvironment, as microglia are responsible for elimination
362 of antigens that threaten the retinal integrity. [38]
363 Microglial activation in the retina is a common feature in various retinal neurodegenerative
364 conditions, including glaucoma and other optic neuropathies. Multiple studies
365 [39] demonstrated the similarity of the activation process across mouse models. To better
366 understand the microglia-RGC interaction and to identify potential therapeutic targets we

367 have built an integrated atlas of mouse retina across conditions. These include
368 developing, healthy adult, optic nerve crush, and microbead-induced glaucoma model.
369 To our knowledge this is the largest integrated atlas containing 1,053,629 cells including
370 36,080 myeloid cells. The downstream analysis highlighted the similarities of the
371 activation process, including the role of the phagocytosis in the elimination of the retinal
372 neurons.

373 Prior studies demonstrated that phosphatidylserine (PS), a phospholipid that is localized
374 to the inner part of the cell membrane, is crucial for identification of apoptotic cells by
375 macrophages. [40,41] Considering donor RGCs experience a substantial stress during
376 dissociation, isolation, and transplantation events, it is predicted they might generate pro-
377 apoptotic signals and externalize a PS signal on the cell surface, allowing them to be
378 recognized and cleared by retinal microglia and macrophages. [42] Annexin V, a calcium-
379 dependent membrane-binding protein, efficiently and specifically attaches to PS, thus,
380 representing a selective probe for recognition and quantification of apoptotic cells. [43–45]
381 By pretreating donor RGCs with annexin V just after isolation and right before
382 transplantation events, a PS signal on the cell surface of donor RGCs can be blocked,
383 hence preventing donor RGCs from being recognized and attacked by retinal microglia
384 and macrophages.

385 In addition to blocking the PS signal with annexin V, we previously demonstrated that
386 treatment with sFasL is also neuroprotective and prevents death of RGCs in chronic and
387 inducible mouse models of glaucoma. [23,46] Herein, we determined the combination of
388 annexin V and sFasL significantly improves survival of donor hRGCs in the host mouse
389 retina. FasL is a type II transmembrane protein that exists as both a membrane bound

390 protein (mFasL) that is pro-inflammatory and pro-apoptotic, and a soluble form (sFasL)
391 that is cleaved from the cell surface and released as a soluble fragment that is non-
392 inflammatory and non-apoptotic and can antagonize the activity of mFasL. [22,23,47] In the
393 healthy eye, the anti-apoptotic and anti-inflammatory sFasL is the dominant isoform
394 expressed, [46] but with disease there is a shift and the pro-inflammatory and pro-apoptotic
395 mFasL is the dominant isoform expressed in a variety of ocular pathologies. [46,48–50]
396 In inducible and chronic models of glaucoma it has been shown that mFasL mediates
397 destruction of RGCs either by directly killing RGCs and/or by inducing the production of
398 pro-inflammatory chemokines or other mediators in Fas^+ glial cells and thereby causing
399 neurotoxic inflammation. [23,46,51] By contrast, intravitreal AAV2-mediated gene delivery of
400 sFasL provided complete and long-term protection of RGCs and their axons. [23,46]
401 Importantly, the sFasL-mediated neuroprotection of RGCs also correlates with reduced
402 microglia activation and reduced production of pro-inflammatory mediators. Therefore,
403 sFasL could be improving survival of donor hRGCs by blocking FasL-mediated apoptosis
404 of RGCs and/or by blocking FasL-mediated activation of glia and the induction of
405 neurotoxic inflammation.
406 Normally, in the healthy eye, retinal microglia display a highly ramified morphology with a
407 small cell body and multiple branching processes. When responding to inflammation or
408 injury, microglia retract their processes and present round cellular morphology. Although
409 microglia are the most abundant immune cells in the retina, the retina also contains a
410 population of perivascular macrophages that are located within the glia limitans of retinal
411 vasculature. [52] The glia limitans acts as a physical barrier against unwanted cells that
412 attempt to enter the retina. During the subretinal delivery of donor hRGCs, the microinjury

413 to small retinal blood vessels may occur causing the leakage of perivascular
414 macrophages to the site of injection. Both microglia and macrophages express the ionized
415 calcium-binding adaptor (Iba1) molecule, a 17-kDa actin-binding cross-linking protein that
416 is upregulated during activation of these cells. [53]
417 Here, we investigated the morphology of Iba1^{+} microglia and macrophages following
418 pretreatment of donor hRGCs with annexin V and sFasL before transplantation. We found
419 that transplantation of donor hRGCs leads to local activation of host retinal microglia and
420 macrophages causing them to move towards the injection site to eliminate donor hRGCs.
421 Pretreatment with annexin V and sFasL resulted in reduced activation of microglia and
422 macrophages, with Iba1^{+} microglia and macrophages displaying a more ramified
423 morphology with longer processes (**Figures 3E, 3F**). In contrast, the Iba1^{+} microglia and
424 macrophages in the control group exhibited a round ameboid morphology with retracted
425 processes (**Figures 3C, 3D**).
426 Our results demonstrate that modulating the host retinal microenvironment through the
427 microglia manipulation can improve the survival of donor hRGCs after transplantation.
428 We believe it might be an important improvement to existing transplantation protocols to
429 other retinal neurons, as well.
430
431 **Statistical analysis**
432 All graphs were generated by GraphPad PRISM 9 (GraphPad software, San Diego, CA).
433 Statistical significance was determined using an unpaired Welch's *t*-test. All data are
434 presented as average ± standard deviation (SD). Where normally distributed, the data

435 were analyzed with a p value of <0.05 (*$p < 0.05$, **$p < 0.01$, ***$p < 0.001$, ****$p < 0.0001$)
436 as a statistically significant.
437

438 **Acknowledgments**

439 This work was supported by NEI/NIH U24 (PB), Gilbert Family Foundation (PB), VRP
440 FTTSA VR220053 (PB), Gilbert Family Foundation (PB). The authors would like to thank
441 Dr. Don Zack for providing the Brn3b-tdTomato hESCs.
442

443 **Author contributions**

444 MHP, VVM, MGK and PB initiated the project and designed experiments. VVM, MHP, JA
445 performed confocal microscopy, immunohistochemistry experiments. JDR differentiated
446 donor hRGCs. JA analyzed the images of microglia cells. EK assembled a single-cell
447 atlas for mouse retina. CA performed scanning laser ophthalmoscopy. VVM and PB
448 performed cell transplantation, wrote the manuscript draft. PB supervised the project. All
449 authors reviewed and contributed to editing the manuscript.
450

451 **Data availability statement**

452 The original code generated in this study is available on GitHub
453 (https://github.com/mcrewcow/Malechka_et_al_2025), and the atlases constructed and
454 utilized in the manuscript are deposited to CELLxGENE
455 (https://cellxgene.cziscience.com/collections/7dd7e8a1-f7c2-4213-9f23-dd52afb7ee16).

456 **Declaration of interests**

457 The authors declare no competing interests.

458 **References:**
459

460 1. Quigley, H.A., and Broman, A.T. (2006). The number of people with glaucoma worldwide in
461 2010 and 2020. Br. J. Ophthalmol. *90*, 262. https://doi.org/10.1136/bjo.2005.081224.

462 2. Cook, C., and Foster, P. (2012). Epidemiology of glaucoma: what's new? Can. J. Ophthalmol.
463 J. Can. d'Ophtalmol. *47*, 223–226. https://doi.org/10.1016/j.jcjo.2012.02.003.

464 3. Newman, N.J., and Biousse, V. (2004). Hereditary optic neuropathies. Eye *18*, 1144–1160.
465 https://doi.org/10.1038/sj.eye.6701591.

466 4. Patil, A.D., Biousse, V., and Newman, N.J. (2022). Ischemic Optic Neuropathies: Current
467 Concepts. Ann. Indian Acad. Neurol. *25*, S54–S58. https://doi.org/10.4103/aian.aian_533_22.

468 5. Klistorner, A., Sriram, P., Vootakuru, N., Wang, C., Barnett, M.H., Garrick, R., Parratt, J.,
469 Levin, N., Raz, N., Walt, A.V. der, et al. (2014). Axonal loss of retinal neurons in multiple
470 sclerosis associated with optic radiation lesions. Neurology *82*, 2165–2172.
471 https://doi.org/10.1212/wnl.0000000000000522.

472 6. Zhang, K.Y., and Johnson, T.V. (2021). The internal limiting membrane: Roles in retinal
473 development and implications for emerging ocular therapies. Exp Eye Res *206*, 108545.
474 https://doi.org/10.1016/j.exer.2021.108545.

475 7. Baranov, P., and Oswald, J. (2018). Retinal Ganglion Cell Replacement: A Bridge to the
476 Brain. In Regenerative Medicine and Stem Cell Therapy for the Eye., pp. 193–206.
477 https://doi.org/10.1007/978-3-319-98080-5_8.

478 8. Shen, J., Xiao, R., Bair, J., Wang, F., Vandenberghe, L.H., Dartt, D., Baranov, P., and Ng,
479 Y.S.E. (2018). Novel engineered, membrane-localized variants of vascular endothelial growth
480 factor (VEGF) protect retinal ganglion cells: a proof-of-concept study. Cell death & disease *9*,
481 1371. https://doi.org/10.1038/s41419-018-1049-0.

482 9. Soucy, J.R., Aguzzi, E.A., Cho, J., Gilhooley, M.J., Keuthan, C., Luo, Z., Monavarfeshani, A.,
483 Saleem, M.A., Wang, X.-W., Wohlschlegel, J., et al. (2023). Retinal ganglion cell repopulation
484 for vision restoration in optic neuropathy: a roadmap from the RReSTORe Consortium. Mol.
485 Neurodegener. *18*, 64. https://doi.org/10.1186/s13024-023-00655-y.

486 10. Singh, M.S., Park, S.S., Albini, T.A., Canto-Soler, M.V., Klassen, H., MacLaren, R.E.,
487 Takahashi, M., Nagiel, A., Schwartz, S.D., and Bharti, K. (2020). Retinal stem cell
488 transplantation: Balancing safety and potential. Prog. Retin. Eye Res. *75*, 100779.
489 https://doi.org/10.1016/j.preteyeres.2019.100779.

490 11. Zhang, J., Wu, S., Jin, Z.-B., and Wang, N. (2021). Stem Cell-Based Regeneration and
491 Restoration for Retinal Ganglion Cell: Recent Advancements and Current Challenges.
492 Biomolecules *11*, 987. https://doi.org/10.3390/biom11070987.

493 12. Venugopalan, P., Wang, Y., Nguyen, T., Huang, A., Muller, K.J., and Goldberg, J.L. (2016).
494 Transplanted neurons integrate into adult retinas and respond to light. Nat. Commun. *7*, 10472.
495 https://doi.org/10.1038/ncomms10472.

496 13. Hertz, J., Qu, B., Hu, Y., Patel, R.D., Valenzuela, D.A., and Goldberg, J.L. (2013). Survival
497 and Integration of Developing and Progenitor-Derived Retinal Ganglion Cells following
498 Transplantation. Cell Transplant. *23*, 855–872. https://doi.org/10.3727/096368913x667024.

499 14. Vrathasha, V., Nikonov, S., Bell, B.A., He, J., Bungatavula, Y., Uyhazi, K.E., and Chavali,
500 V.R.M. (2022). Transplanted human induced pluripotent stem cells- derived retinal ganglion
501 cells embed within mouse retinas and are electrophysiologically functional. iScience *25*, 105308.
502 https://doi.org/10.1016/j.isci.2022.105308.

503 15. Rashid, K., Akhtar-Schaefer, I., and Langmann, T. (2019). Microglia in Retinal
504 Degeneration. Front. Immunol. *10*, 1975. https://doi.org/10.3389/fimmu.2019.01975.

505 16. Karlstetter, M., Scholz, R., Rutar, M., Wong, W.T., Provis, J.M., and Langmann, T. (2015).
506 Retinal microglia: Just bystander or target for therapy? Prog. Retin. Eye Res. *45*, 30–57.
507 https://doi.org/10.1016/j.preteyeres.2014.11.004.

508 17. Chen, M., and Xu, H. (2015). Parainflammation, chronic inflammation, and age-related
509 macular degeneration. J. Leucoc. Biol. *98*, 713–725. https://doi.org/10.1189/jlb.3ri0615-239r.

510 18. Pan, L., Cho, K.-S., Wei, X., Xu, F., Lennikov, A., Hu, G., Tang, J., Guo, S., Chen, J.,
511 Kriukov, E., et al. (2023). IGFBPL1 is a master driver of microglia homeostasis and resolution of
512 neuroinflammation in glaucoma and brain tauopathy. Cell Rep. *42*, 112889.
513 https://doi.org/10.1016/j.celrep.2023.112889.

514 19. Vermes, I., Haanen, C., Steffens-Nakken, H., and Reutellingsperger, C. (1995). A novel
515 assay for apoptosis Flow cytometric detection of phosphatidylserine expression on early
516 apoptotic cells using fluorescein labelled Annexin V. J. Immunol. Methods *184*, 39–51.
517 https://doi.org/10.1016/0022-1759(95)00072-i.

518 20. Kägi, D., Vignaux, F., Ledermann, B., Bürki, K., Depraetere, V., Nagata, S., Hengartner, H.,
519 and Golstein, P. (1994). Fas and Perforin Pathways as Major Mechanisms of T Cell-Mediated
520 Cytotoxicity. Science *265*, 528–530. https://doi.org/10.1126/science.7518614.

521 21. Suda, T., Hashimoto, H., Tanaka, M., Ochi, T., and Nagata, S. (1997). Membrane Fas Ligand
522 Kills Human Peripheral Blood T Lymphocytes, and Soluble Fas Ligand Blocks the Killing. J.
523 Exp. Med. *186*, 2045–2050. https://doi.org/10.1084/jem.186.12.2045.

524 22. Hohlbaum, A.M., Moe, S., and Marshak-Rothstein, A. (2000). Opposing Effects of
525 Transmembrane and Soluble FAS Ligand Expression on Inflammation and Tumor Cell Survival.
526 J. Exp. Med. *191*, 1209–1220. https://doi.org/10.1084/jem.191.7.1209.

527 23. Gregory, M.S., Hackett, C.G., Abernathy, E.F., Lee, K.S., Saff, R.R., Hohlbaum, A.M.,
528 Moody, K.L., Hobson, M.W., Jones, A., Kolovou, P., et al. (2011). Opposing Roles for
529 Membrane Bound and Soluble Fas Ligand in Glaucoma-Associated Retinal Ganglion Cell Death.
530 PLoS ONE *6*, e17659. https://doi.org/10.1371/journal.pone.0017659.

531 24. Rogge, M., Yin, X.-T., Godfrey, L., Lakireddy, P., Potter, C.A., Rosso, C.R.D., and Stuart,
532 P.M. (2015). Therapeutic Use of Soluble Fas Ligand Ameliorates Acute and Recurrent Herpetic
533 Stromal Keratitis in Mice. Investig. Opthalmology Vis. Sci. *56*, 6377.
534 https://doi.org/10.1167/iovs.15-16588.

535 25. Li, N.-L., Nie, H., Yu, Q.-W., Zhang, J.-Y., Ma, A.-L., Shen, B.-H., Wang, L., Bai, J., Chen,
536 X.-H., Zhou, T., et al. (2004). Role of soluble Fas ligand in autoimmune diseases. World J.
537 Gastroenterol. *10*, 3151–3156. https://doi.org/10.3748/wjg.v10.i21.3151.

538 26. Fligor, C.M., Huang, K.-C., Lavekar, S.S., VanderWall, K.B., and Meyer, J.S. (2020).
539 Differentiation of retinal organoids from human pluripotent stem cells. Methods Cell Biol. *159*,
540 279–302. https://doi.org/10.1016/bs.mcb.2020.02.005.

541 27. Oswald, J., Kegeles, E., Minelli, T., Volchkov, P., and Baranov, P. (2021). Transplantation of
542 miPSC/mESC-derived retinal ganglion cells into healthy and glaucomatous retinas. Mol. Ther. -
543 Methods Clin. Dev. *21*, 180–198. https://doi.org/10.1016/j.omtm.2021.03.004.

544 28. Soucy, J.R., Todd, L., Kriukov, E., Phay, M., Malechka, V.V., Rivera, J.D., Reh, T.A., and
545 Baranov, P. (2023). Controlling donor and newborn neuron migration and maturation in the eye
546 through microenvironment engineering. Proc. Natl. Acad. Sci. *120*, e2302089120.
547 https://doi.org/10.1073/pnas.2302089120.

548 29. Young, K., and Morrison, H. (2018). Quantifying Microglia Morphology from
549 Photomicrographs of Immunohistochemistry Prepared Tissue Using ImageJ. J. Vis. Exp. : JoVE,
550 57648. https://doi.org/10.3791/57648.

551 30. Alt, C., and Lin, C.P. (2012). In vivo quantification of microglia dynamics with a scanning
552 laser ophthalmoscope in a mouse model of focal laser injury. Ophthalmic Technol. XXII,
553 820907-820907–820909. https://doi.org/10.1117/12.909141.

554 31. O'Koren, E.G., Yu, C., Klingeborn, M., Wong, A.Y.W., Prigge, C.L., Mathew, R.,
555 Kalnitsky, J., Msallam, R.A., Silvin, A., Kay, J.N., et al. (2019). Microglial Function Is Distinct
556 in Different Anatomical Locations during Retinal Homeostasis and Degeneration. Immunity *50*,
557 723-737.e7. https://doi.org/10.1016/j.immuni.2019.02.007.

558 32. Carelli, V., Morgia, C.L., Ross-Cisneros, F.N., and Sadun, A.A. (2017). Optic neuropathies:
559 the tip of the neurodegeneration iceberg. Hum. Mol. Genet. *26*, R139–R150.
560 https://doi.org/10.1093/hmg/ddx273.

561 33. Johnson, T.V., Bull, N.D., Hunt, D.P., Marina, N., Tomarev, S.I., and Martin, K.R. (2010).
562 Neuroprotective Effects of Intravitreal Mesenchymal Stem Cell Transplantation in Experimental
563 Glaucoma. Investig. Opthalmology Vis. Sci. *51*, 2051. https://doi.org/10.1167/iovs.09-4509.

564 34. Chamling, X., Sluch, V.M., and Zack, D.J. (2016). The Potential of Human Stem Cells for
565 the Study and Treatment of Glaucoma. Investig. Ophthalmol. Vis. Sci. *57*, ORSFi1–ORSFi6.
566 https://doi.org/10.1167/iovs.15-18590.

567 35. Silva-Junior, A.J. da, Mesentier-Louro, L.A., Nascimento-dos-Santos, G., Teixeira-Pinheiro,
568 L.C., Vasques, J.F., Chimeli-Ormonde, L., Bodart-Santos, V., Carvalho, L.R.P. de, Santiago,
569 M.F., and Mendez-Otero, R. (2021). Human mesenchymal stem cell therapy promotes retinal
570 ganglion cell survival and target reconnection after optic nerve crush in adult rats. Stem Cell Res.
571 Ther. *12*, 69. https://doi.org/10.1186/s13287-020-02130-7.

572 36. Chang, E.E., and Goldberg, J.L. (2011). Glaucoma 2.0: neuroprotection, neuroregeneration,
573 neuroenhancement. Ophthalmology *119*, 979–986. https://doi.org/10.1016/j.ophtha.2011.11.003.

574 37. Wareham, L.K., Risner, M.L., and Calkins, D.J. (2020). Protect, Repair, and Regenerate:
575 Towards Restoring Vision in Glaucoma. Curr. Ophthalmol. Rep. *8*, 301–310.
576 https://doi.org/10.1007/s40135-020-00259-5.

577 38. Murenu, E., Gerhardt, M.-J., Biel, M., and Michalakis, S. (2022). More than meets the eye:
578 The role of microglia in healthy and diseased retina. Front. Immunol. *13*, 1006897.
579 https://doi.org/10.3389/fimmu.2022.1006897.

580 39. Fan, W., Huang, W., Chen, J., Li, N., Mao, L., and Hou, S. (2022). Retinal microglia:
581 Functions and diseases. Immunology *166*, 268–286. https://doi.org/10.1111/imm.13479.

582 40. Fadok, V.A., Savill, J.S., Haslett, C., Bratton, D.L., Doherty, D.E., Campbell, P.A., and
583 Henson, P.M. (1992). Different populations of macrophages use either the vitronectin receptor or
584 the phosphatidylserine receptor to recognize and remove apoptotic cells. J. Immunol. *149*, 4029–
585 4035. https://doi.org/10.4049/jimmunol.149.12.4029.

586 41. Martin, S.J., Reutelingsperger, C.P., McGahon, A.J., Rader, J.A., Schie, R.C. van, LaFace,
587 D.M., and Green, D.R. (1995). Early redistribution of plasma membrane phosphatidylserine is a
588 general feature of apoptosis regardless of the initiating stimulus: inhibition by overexpression of
589 Bcl-2 and Abl. J. Exp. Med. *182*, 1545–1556. https://doi.org/10.1084/jem.182.5.1545.

590 42. Logue, S.E., Elgendy, M., and Martin, S.J. (2009). Expression, purification and use of
591 recombinant annexin V for the detection of apoptotic cells. Nat. Protoc. *4*, 1383–1395.
592 https://doi.org/10.1038/nprot.2009.143.

593 43. Gerke, V. (2001). Annexins And Membrane Organisation In The Endocytic Pathway. Cell.
594 Mol. Biol. Lett. *6*, 204.

595 44. Gerke, V., and Moss, S.E. (2002). Annexins: From Structure to Function. Physiol. Rev. *82*,
596 331–371. https://doi.org/10.1152/physrev.00030.2001.

597 45. Koopman, G., Reutelingsperger, C., Kuijten, G., Keehnen, R., Pals, S., and Oers, M. van
598 (1994). Annexin V for flow cytometric detection of phosphatidylserine expression on B cells
599 undergoing apoptosis. Blood *84*, 1415–1420.
600 https://doi.org/10.1182/blood.v84.5.1415.bloodjournal8451415.

601 46. Krishnan, A., Fei, F., Jones, A., Busto, P., Marshak-Rothstein, A., Ksander, B.R., and
602 Gregory-Ksander, M. (2016). Overexpression of Soluble Fas Ligand following Adeno-
603 Associated Virus Gene Therapy Prevents Retinal Ganglion Cell Death in Chronic and Acute
604 Murine Models of Glaucoma. J. Immunol. *197*, 4626–4638.
605 https://doi.org/10.4049/jimmunol.1601488.

606 47. Tanaka, M., Itai, T., Adachi, M., and Nagata, S. (1998). Downregulation of Fas ligand by
607 shedding. Nat. Med. *4*, 31–36. https://doi.org/10.1038/nm0198-031.

608 48. Gregory, M.S., Repp, A.C., Holhbaum, A.M., Saff, R.R., Marshak-Rothstein, A., and
609 Ksander, B.R. (2002). Membrane Fas Ligand Activates Innate Immunity and Terminates Ocular
610 Immune Privilege. J. Immunol. *169*, 2727–2735. https://doi.org/10.4049/jimmunol.169.5.2727.

611 49. Matsumoto, H., Murakami, Y., Kataoka, K., Notomi, S., Mantopoulos, D., Trichonas, G.,
612 Miller, J.W., Gregory, M.S., Ksander, B.R., Marshak-Rothstein, A., et al. (2015). Membrane-
613 bound and soluble Fas ligands have opposite functions in photoreceptor cell death following
614 separation from the retinal pigment epithelium. Cell Death Dis. *6*, e1986.
615 https://doi.org/10.1038/cddis.2015.334.

616 50. Gregory-Ksander, M., Perez, V.L., Marshak-Rothstein, A., and Ksander, B.R. (2019).
617 Soluble Fas ligand blocks destructive corneal inflammation in mouse models of corneal
618 epithelial debridement and LPS induced keratitis. Exp. Eye Res. *179*, 47–54.
619 https://doi.org/10.1016/j.exer.2018.10.013.

620 51. Krishnan, A., Kocab, A.J., Zacks, D.N., Marshak-Rothstein, A., and Gregory-Ksander, M.
621 (2019). A small peptide antagonist of the Fas receptor inhibits neuroinflammation and prevents
622 axon degeneration and retinal ganglion cell death in an inducible mouse model of glaucoma. J.
623 Neuroinflammation *16*, 184. https://doi.org/10.1186/s12974-019-1576-3.

624 52. Mendes-Jorge, L., Ramos, D., Luppo, M., Llombart, C., Alexandre-Pires, G., Nacher, V.,
625 Melgarejo, V., Correia, M., Navarro, M., Carretero, A., et al. (2009). Scavenger function of
626 resident autofluorescent perivascular macrophages and their contribution to the maintenance of
627 the blood-retinal barrier. Investig. Ophthalmol. Vis. Sci. *50*, 5997–6005.
628 https://doi.org/10.1167/iovs.09-3515.

629 53. Sasaki, Y., Ohsawa, K., Kanazawa, H., Kohsaka, S., and Imai, Y. (2001). Iba1 Is an Actin-
630 Cross-Linking Protein in Macrophages/Microglia. Biochem. Biophys. Res. Commun. *286*, 292–
631 297. https://doi.org/10.1006/bbrc.2001.5388.

632

633 **Figure legends:**

634 **Figure 1.** Donor cell survival is improved by blocking phosphatidylcholine (PS) residues
635 on human donor retinal ganglion cells (hRGCs) with annexin V. (**A**) Donor hRGCs survive
636 and send their projections to the optic nerve head (ONH). (**B**) Donor hRGCs survive better
637 after pretreatment with annexin V. (**C**) Donor hRGCs enter ONH more successfully after
638 pretreatment with annexin V.

639 **Figure 2.** Studying microglia activation *in vivo* in the retina of *Cx3cr1-GFP* mice after
640 donor human retinal ganglion cells (hRGCs) transplantation. (**A**) Imaging *in vivo* by
641 scanning laser ophthalmoscopy (SLO). Image on day 1 represents injected donor
642 tdTomato$^+$ hRGCs (red) and host microglia cells (green) after transplantation. Note that
643 by day 7 all injected donor tdTomato$^+$ hRGCs are eliminated by activated host microglia
644 cells. (**B**) Interaction between host microglia and donor hRGCs on a single cell level. (**C**)
645 Morphological characteristics of a microglia cell. Scale bar: 5 μm

646 **Figure 3.** Pretreatment of donor hRGCs with annexin V and sFasL inhibits microglia
647 activation and increases survival of donor hRGCs after transplantation. (**A, B**) Donor
648 hRGCs survive better after pretreatment with annexin V and sFasL. Activation of Iba1-
649 positive microglia and macrophages in the OPL (**C, E**) and IPL (**D, F**) of the retina in the
650 control group and group pretreated with annexin V and sFasL before donor hRGC
651 transplantation. Microglia density (**G, J**), number of branches per microglia and
652 macrophage cell (**H, K**), branch length per microglia and macrophage cell (**I, L**) in the
653 OPL (**G, H, I**) and IPL (**J, K, L**) of the retina in the control group and group pretreated with

654 annexin V and sFasL. hRGCs, human retinal ganglion cells; IPL, inner plexiform layer;
655 OPL, outer plexiform layer; sFasL, soluble Fas ligand.

656 **Figure 4.** (**A**) Integrated dataset of mouse developing (E10-P8), healthy adult (4 - 52
657 weeks), microbeads-induced glaucoma, and optic nerve crush retinal myeloid population.
658 (**B**) Heatmap demonstrating expression patterns of classical microglia-related genes
659 between the conditions. (**C**) Pathway analysis demonstrates condition-specific, and
660 microglia activation related signaling patterns between the conditions. Distribution of
661 *Apoe* expression in the integrated dataset (**D**) and between the conditions (**E**). (**F**) Chart
662 highlighting the differences in percentage of *Apoe*$^+$ (expression >= 4) cells between the
663 conditions.
664 (**G**) Dynamics of Apoe expression between the conditions for the total dataset (bottom)
665 and *Apoe*$^+$ (expression >= 4) cells. E, embryonic day; P, postnatal day.

666 **Figure 5.** (**A**) Integrated dataset of mouse developing (E10-P8), healthy adult (4 - 52
667 weeks), and optic nerve crush retinal ganglion cell population. (**B**) Heatmap
668 demonstrating expression patterns of known “eat-me”, “do-not-eat-me”, and “find-me”
669 genes between the conditions. E, embryonic day; P, postnatal day.

670

671 **Supplementary figure legends.**

672 **Figure 1.** Elimination of donor human retinal ganglion cells (hRGCs) by primary microglia
673 *in vitro* on day 0 (**A**) and day 1 (**B**).

674

675

676

677 **Supplementary Table 1.**

678

GSE	DOI	Condition
GSE123758	Not published_3, as in CELLxGENE	Mouse healthy adult retina atlas
GSE125708	10.1073/pnas.1821122116 (https://pubmed.ncbi.nlm.nih.gov/30988181/)	Mouse healthy adult retina atlas
GSE132229	10.1073/pnas.1915571116 (https://pubmed.ncbi.nlm.nih.gov/31843893/)	Mouse healthy adult retina atlas
GSE137398	10.1016/j.neuron.2019.11.006 (https://pubmed.ncbi.nlm.nih.gov/31784286/)	Mouse healthy adult retina atlas
GSE137828	10.1016/j.neuron.2019.11.006 (https://pubmed.ncbi.nlm.nih.gov/31784286/)	Mouse healthy adult retina atlas
GSE153674	PMID: 33088174 (https://pubmed.ncbi.nlm.nih.gov/33088174/)	Mouse healthy adult retina atlas
GSE164044	10.1016/i.neuron.2019.08.002 (https://pubmed.ncbi.nlm.nih.gov/31493975/)	Mouse healthy adult retina atlas
GSE169262	10.1038/s41467-021-27924-y (https://pubmed.ncbi.nlm.nih.gov/35017532/)	Mouse healthy adult retina atlas
GSE176204	10.1016/i.celrep.2023.112889 (https://pubmed.ncbi.nlm.nih.gov/37527036/)	Mouse healthy adult retina atlas
GSE183572	10.1038/s42003-022-03676-3 (https://www.nature.com/articles/s42003-022-03676-3)	Mouse healthy adult retina atlas
GSE199317	10.1038/s41590-023-01437-w (https://pubmed.ncbi.nlm.nih.gov/36807640/)	Mouse healthy adult retina atlas
GSE204880	10.1038/s42003-023-05300-4 (https://pubmed.ncbi.nlm.nih.gov/37670124/)	Mouse healthy adult retina atlas
GSE205123	10.1016/j.ygeno.2023.110644 (https://pubmed.ncbi.nlm.nih.gov/37279838/)	Mouse healthy adult retina atlas
GSE220626	10.3389/fcell.2023.1252547 (https://pubmed.ncbi.nlm.nih.gov/37691820/)	Mouse healthy adult retina atlas
GSE232470	10.1186/s40478-023-01580-3 (https://pubmed.ncbi.nlm.nih.gov/37226256/)	Mouse healthy adult retina atlas
GSE236389	Not published_1, as in CELLxGENE	Mouse healthy adult retina atlas
GSE239347	10.1073/pnas.2314698120 (https://pubmed.ncbi.nlm.nih.gov/38064509/)	Mouse healthy adult retina atlas
GSE243100	10.2337/db23-0368 (https://pubmed.ncbi.nlm.nih.gov/37976214/)	Mouse healthy adult retina atlas
GSE243413	10.1016/i.isci.2024.109916 (https://pubmed.ncbi.nlm.nih.gov/38812536/)	Mouse healthy adult retina atlas
GSE251717	10.1101/2024.03.18.585452 (https://pubmed.ncbi.nlm.nih.gov/38562864/)	Mouse healthy adult retina atlas
GSE263877	10.1038/s41467-024-50033-5 (https://pubmed.ncbi.nlm.nih.gov/39009597/)	Mouse healthy adult retina atlas
GSE137398	10.1016/i.neuron.2019.11.006 (https://pubmed.ncbi.nlm.nih.gov/31784286/)	Mouse optic nerve crush retina

GSE199317	10.1038/s41590-023-01437-w (https://pubmed.ncbi.nlm.nih.gov/36807640/)	Mouse optic nerve crush retina
GSE201254	10.1016/i.neuron.2022.06.002 (https://pubmed.ncbi.nlm.nih.gov/35767994/)	Mouse optic nerve crush retina
GSE206622	10.1016/j.neuron.2022.06.022 (https://pubmed.ncbi.nlm.nih.gov/35952672/)	Mouse optic nerve crush retina
GSE206623	10.1016/j.neuron.2022.06.022 (https://pubmed.ncbi.nlm.nih.gov/35952672/)	Mouse optic nerve crush retina
GSE206624	10.1016/j.neuron.2022.06.022 (https://pubmed.ncbi.nlm.nih.gov/35952672/)	Mouse optic nerve crush retina
GSE206625	10.1016/j.neuron.2022.06.022 (https://pubmed.ncbi.nlm.nih.gov/35952672/)	Mouse optic nerve crush retina
GSE223530	10.1073/pnas.2305947121 (https://pubmed.ncbi.nlm.nih.gov/38289952/)	Mouse optic nerve crush retina
GSE228627	10.1101/2023.11.17.567614 (https://pubmed.ncbi.nlm.nih.gov/38014168/)	Mouse optic nerve crush retina
GSE232470	10.1186/s40478-023-01580-3 (https://pubmed.ncbi.nlm.nih.gov/37226256/)	Mouse optic nerve crush retina
GSE241268	10.1038/s41467-024-46428-z (https://pubmed.ncbi.nlm.nih.gov/38467611/)	Mouse optic nerve crush retina
GSE248537	10.1038/s41467-024-46428-z (https://pubmed.ncbi.nlm.nih.gov/38467611/)	Mouse optic nerve crush retina
GSE226456	10.1016/i.celrep.2023.112889 (https://pubmed.ncbi.nlm.nih.gov/37527036/)	Mouse MB-induced glaucoma retina
GSE247776	10.1038/s41467-024-50050-4 (https://pubmed.ncbi.nlm.nih.gov/39080269/)	Mouse MB-induced glaucoma retina
not published	not published, as in CELLxGENE (Dong Feng Chen Lab)	Mouse MB-induced glaucoma retina
GSE118614	10.1016/i.neuron.2019.04.010 (https://pubmed.ncbi.nlm.nih.gov/31128945/)	Mouse healthy developing retina
GSE122466	10.1242/dev.178103 (https://pubmed.ncbi.nlm.nih.gov/31399471/)	Mouse healthy developing retina
GSE139904	10.1126/sciadv.abj9846 (https://pubmed.ncbi.nlm.nih.gov/34757798/)	Mouse healthy developing retina
GSE186069	10.1038/s41586-024-07069-w (https://pubmed.ncbi.nlm.nih.gov/38947520/)	Mouse healthy developing retina
GSE172101	10.1242/dev.199399 (https://pubmed.ncbi.nlm.nih.gov/34143204/)	Mouse healthy developing retina
GSE202734	10.1016/j.celrep.2023.112237 (https://pubmed.ncbi.nlm.nih.gov/36924502/)	Mouse healthy developing retina
GSE222956	10.1016/j.celrep.2023.112237 (https://pubmed.ncbi.nlm.nih.gov/36924502/)	Mouse healthy developing retina
GSE228590	10.1038/s41586-024-07069-w (https://pubmed.ncbi.nlm.nih.gov/38947520/)	Mouse healthy developing retina
GSE245542	10.1016/i.celrep.2024.114291 (https://pubmed.ncbi.nlm.nih.gov/38823017/)	Mouse healthy developing retina
GSE252861	10.1016/i.isci.2024.110100 (https://pubmed.ncbi.nlm.nih.gov/38947520/)	Mouse healthy developing retina

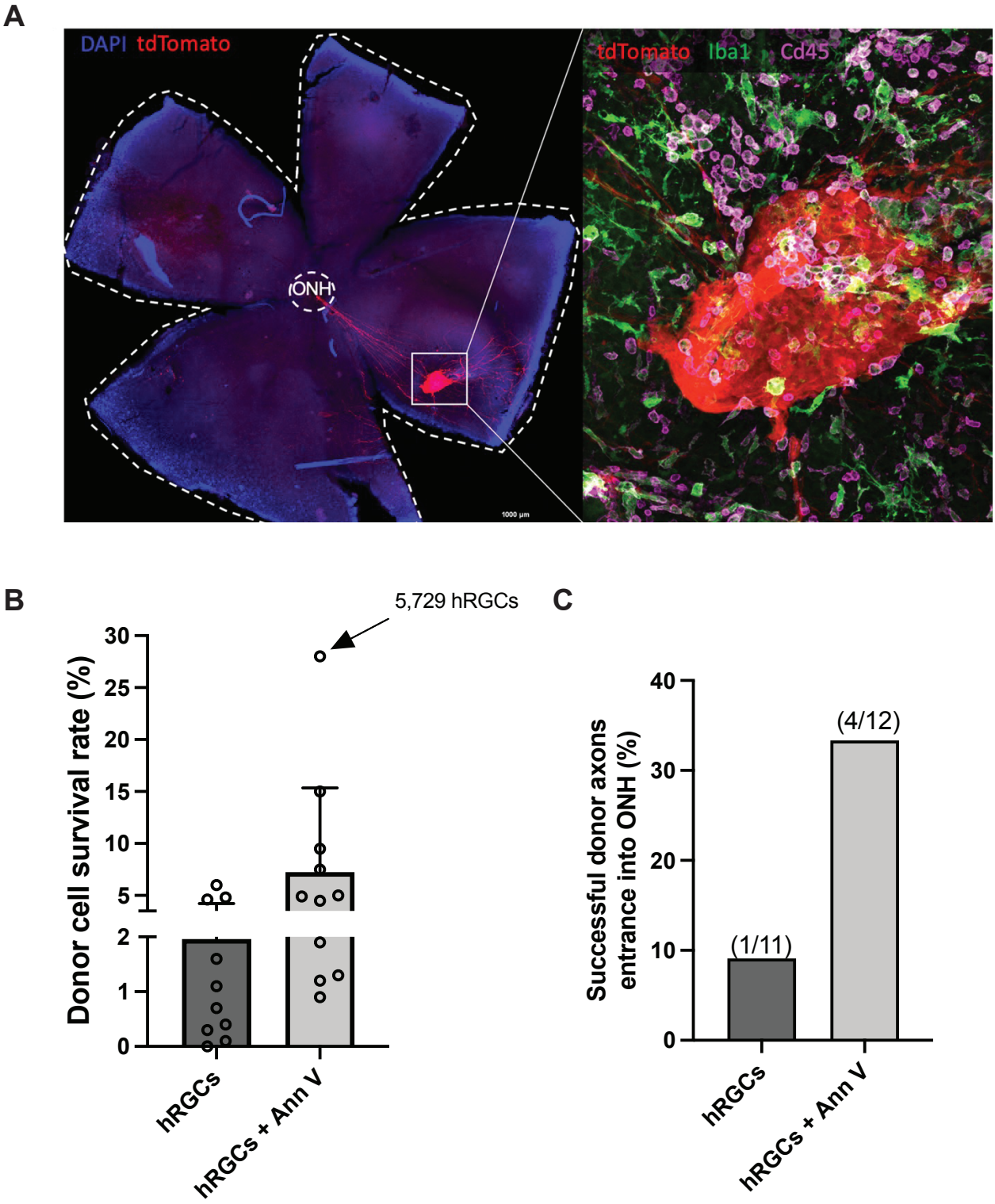

Figure 1. Malechka VV et al. 2025

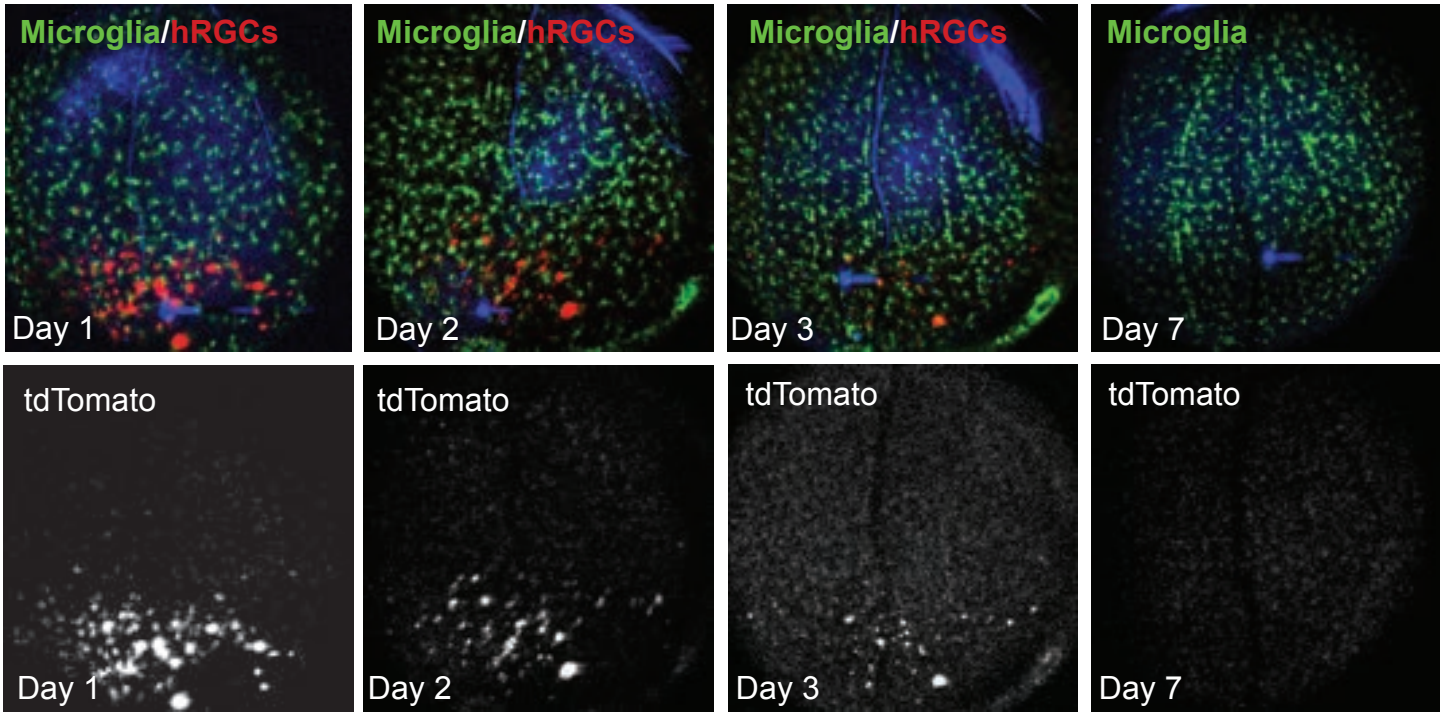

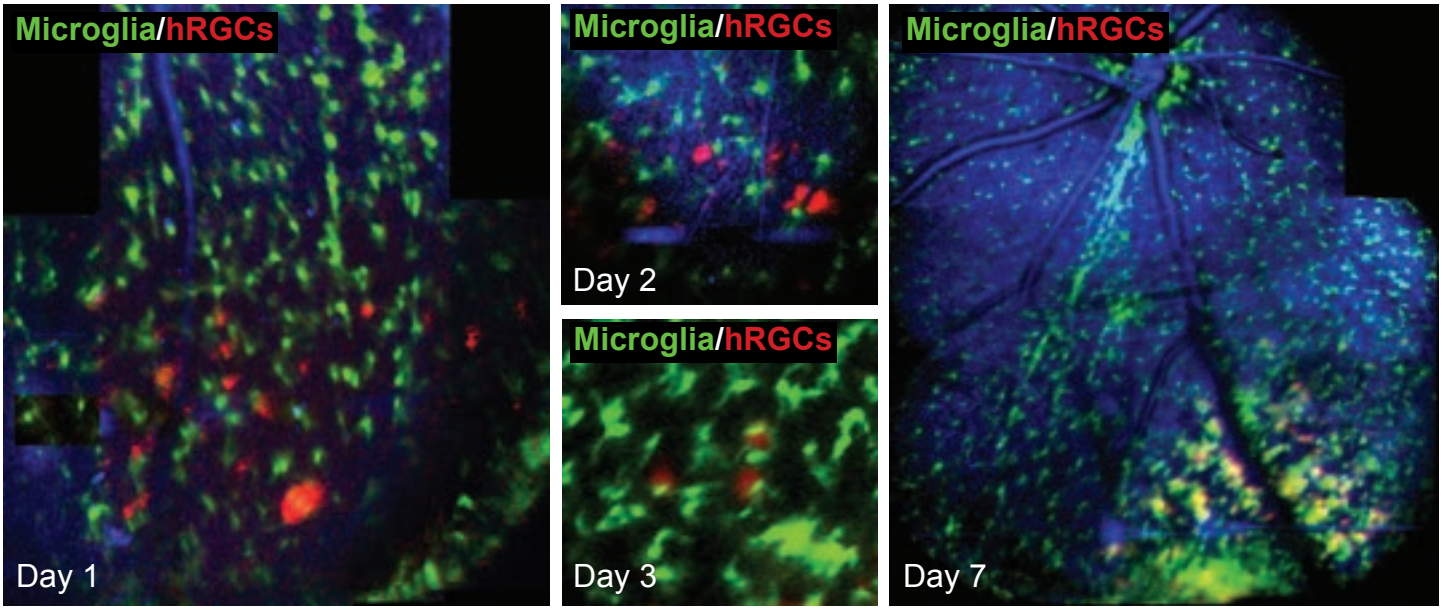

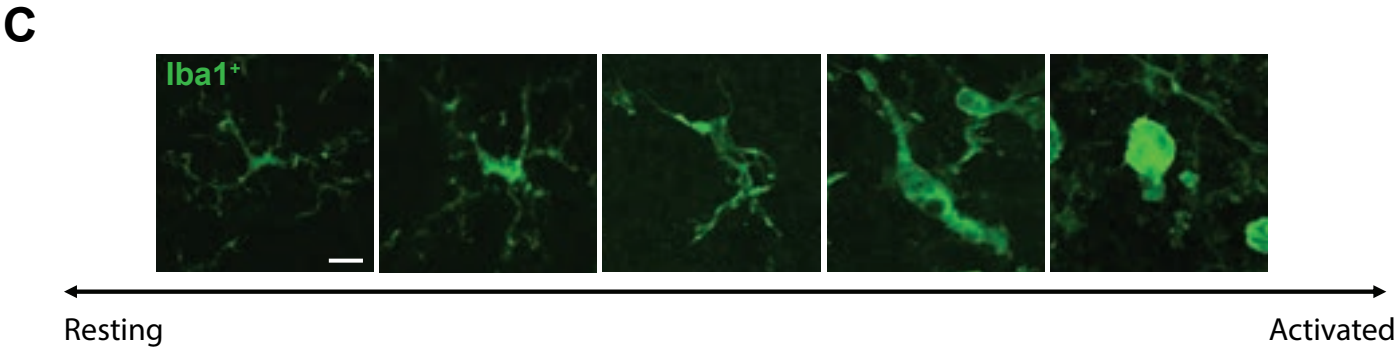

Figure 2. Malechka VV et al. 2025

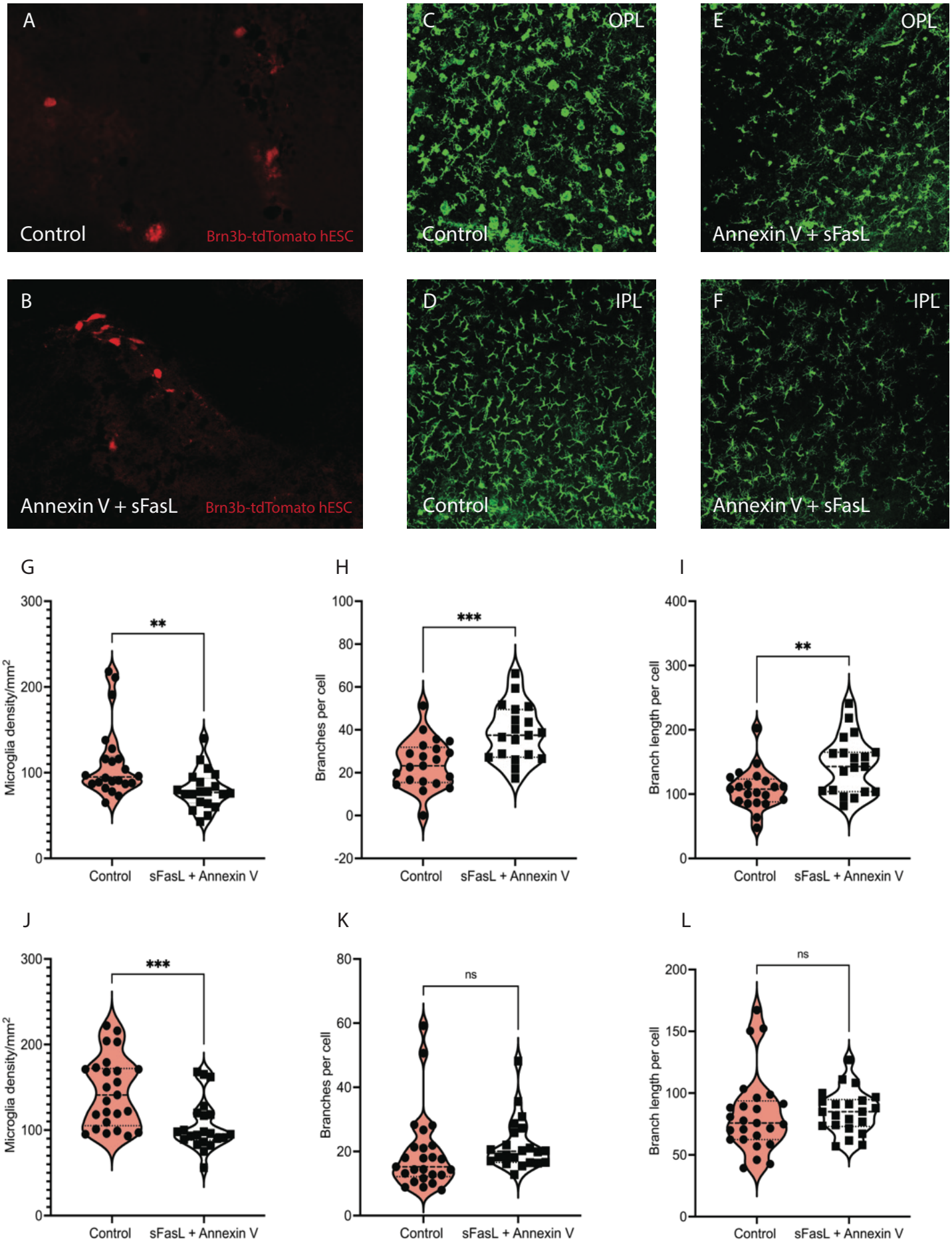

Figure 4. Malechka VV et al. 2024

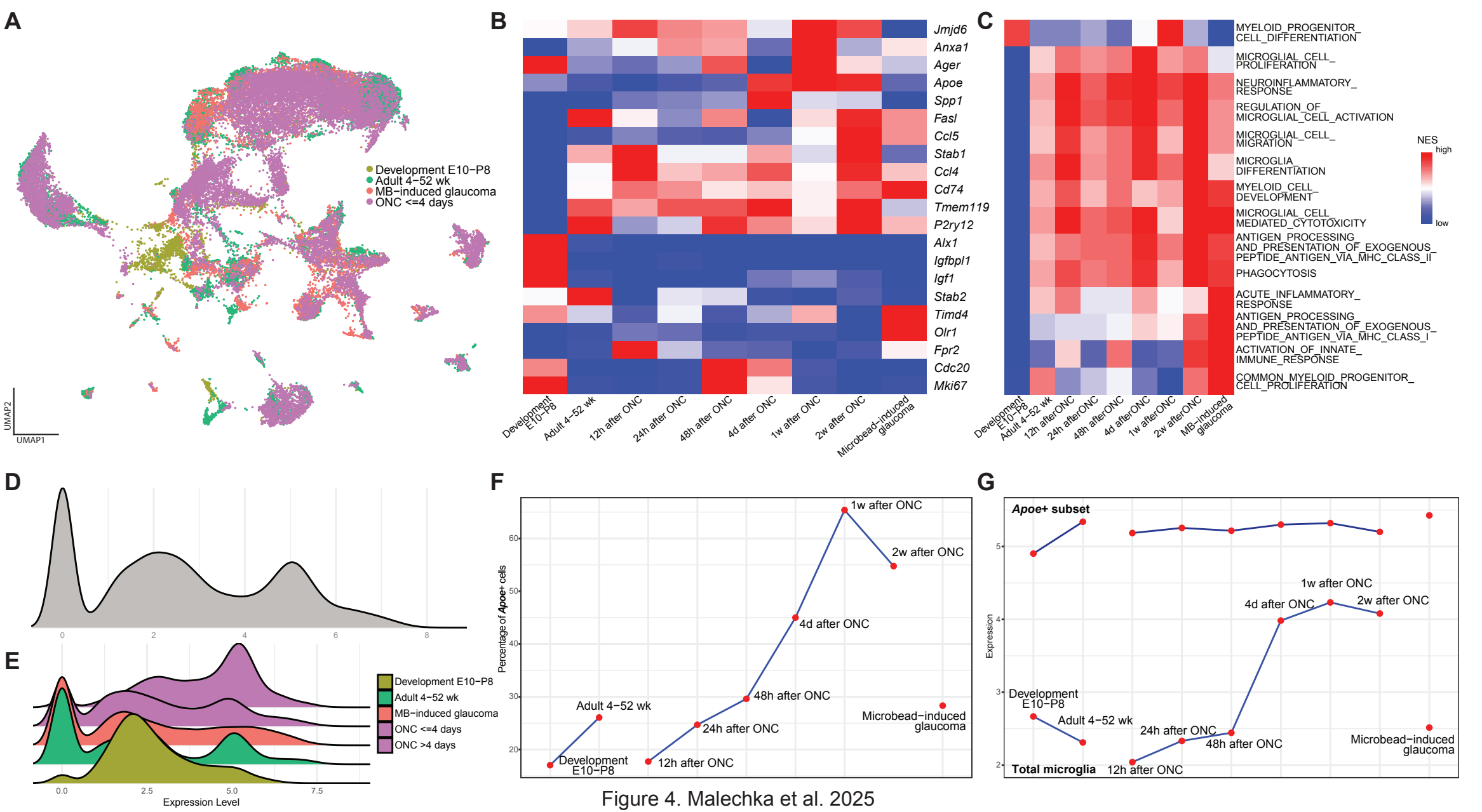

Figure 4. Malechka et al. 2025

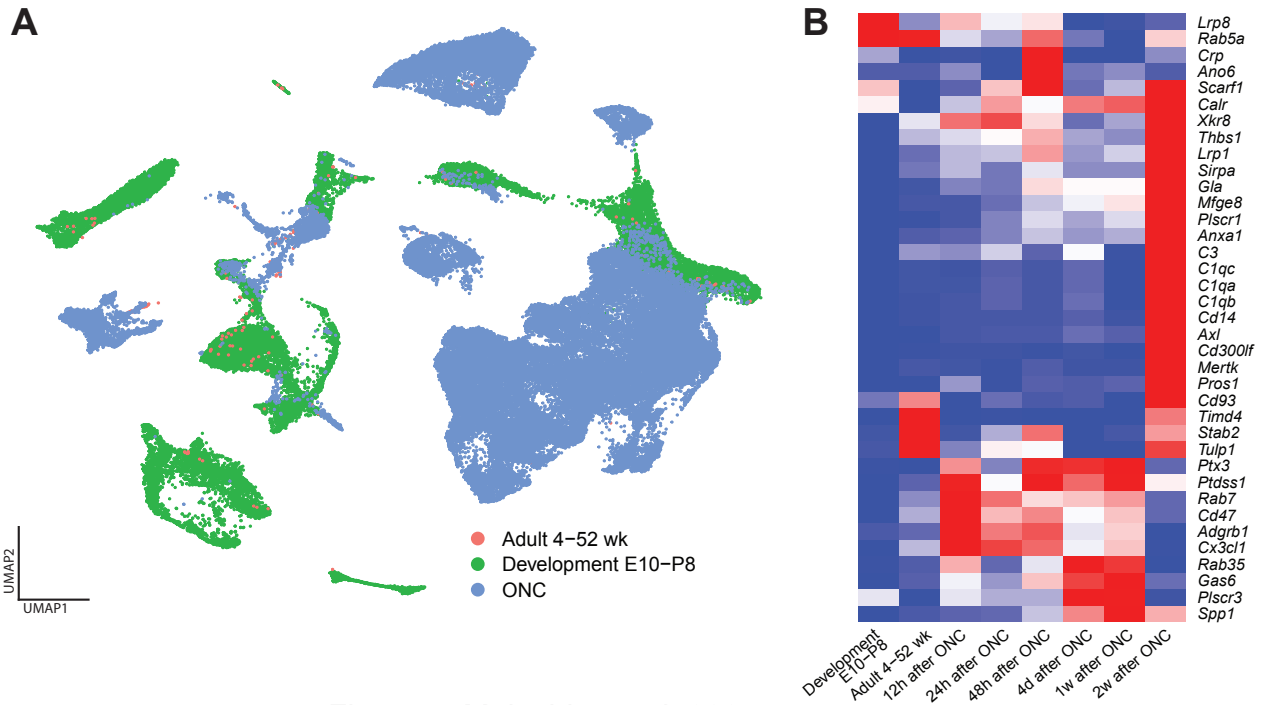

Figure 5. Malechka et al. 2025